Available online at www.sciencedirect.com

ScienceDirect

Nuclear Physics A 967 (2017) 468–471

NUCLEAR PHYSICS A

www.elsevier.com/locate/nuclphysa

Azimuthally differential pion femtoscopy relative to the second and third harmonic in Pb–Pb 2.76 TeV collision from ALICE

Mohammad Saleh (for the ALICE Collaboration)

Wayne State University, 42 W. Warren Ave, Detroit, MI 48202

Abstract

Azimuthally differential femtoscopic measurements, being sensitive to spatio-temporal characteristics of the source as well as to the collective velocity fields at freeze-out, provide very important information on the nature and dynamics of the system evolution. While the HBT radii modulations relative to the second harmonic event plane reflect mostly the spatial geometry of the source, the third harmonic results are mostly defined by the velocity fields [1]. Radii variations with respect to the third harmonic event plane unambiguously signal a collective expansion and anisotropy in the flow fields. Event shape engineering (ESE) is a technique proposed to select events corresponding to a particular shape. Azimuthally differential HBT combined with ESE allows for a detailed analysis of the relation between initial geometry, anisotropic flow and the deformation of source shape. We present azimuthally differential pion femtoscopy with respect to second and third harmonic event planes as a function of the pion transverse momentum for different collision centralities in Pb–Pb collisions at $\sqrt{s_{\rm NN}}$ = 2.76 TeV. All these results are compared to existing models. The effects of the selection of the events with high elliptic or triangular flow are also presented.

Keywords: LHC, ALICE, HBT, femtoscopy, final eccentricity, elliptic shape, freeze-out, Azimuthally differential

1. Introduction

The correlation of two identical particles at small relative momentum, commonly known as intensity, or Hanbury Brown-Twiss (HBT), interferometry, is an effective tool to study the space-time structure of the emitting source in relativistic heavy-ion collisions [2]. Due to the position-momentum correlations in particle emission, the so-called HBT radii become sensitive to the collective velocity fields, from which information about the dynamics of the system evolution can be extracted. Azimuthally differential femtoscopic measurements can be performed relative to the direction of different harmonic flow planes [3]. In particular, measurements of the HBT radii relative to the second harmonic flow provide information on the final shape of the system, which is expected to become more spherical compared to the initial state due to stronger in-plane expansion. In contrast, the azimuthal dependence of the HBT radii relative to the third harmonic flow plane can originate only from the the anisotropies in collective flow gradients, and the observation of any HBT radii azimuthal dependence will unambiguously signals a collective expansion and anisotropy in the flow fields [1]. Event shape engineering (ESE) is a relatively new technique which selects on the magnitude of the flow vector [4]. This selection can provide more control on the initial shape of the source.

http://dx.doi.org/10.1016/j.nuclphysa.2017.07.011

2. Experimental analysis and results

The data Pb–Pb data used in this analysis were collected by ALICE in 2011. The Time Projection Chamber (TPC) was used to reconstruct the tracks in the pseudorapidity range $|\eta| < 0.8$ as well as to identify pions. In addition to the TPC, the Time-Of-Flight (TOF) detector was used for identifying pions. The second and third harmonic event plane angles, Ψ_2 and Ψ_3, were determined from the event plane method [5] using TPC tracks. To avoid self-correlation, each event was split into two subevents ($-0.8 < \eta < 0$ and $0 < \eta < 0.8$). Pairs were chosen from one subevent and the event-plane angle was determined using the other subevent particles, and vice-versa, with the event plane resolution determined from the correlation between the event planes determined in different subevents [5].

The correlation function $C(\mathbf{q})$ was calculated as the ratio of $A(\mathbf{q})$ and $B(\mathbf{q})$, where $\mathbf{q} = \mathbf{p}_1 - \mathbf{p}_2$ is the relative 3-momentum of two pions, $A(\mathbf{q})$ is the same-event distribution of particle pairs, and $B(\mathbf{q})$ is the background distribution of uncorrelated particle pairs obtained using mixed events technique. The Bertsch-Pratt [6] out–side–long coordinate system was used with the *long* direction pointing along the beam axis, *out* along the transverse pair momentum, and *side* being perpendicular to the other two. The correlation function is fitted to

$$C(\mathbf{q}, \Delta\varphi) = N[(1 - \lambda) + \lambda K(\mathbf{q})(1 + G(\mathbf{q}, \Delta\varphi))], \tag{1}$$

where N is the normalization factor, λ is the chaoticity, and $\Delta\varphi = \varphi_{\text{pair}} - \Psi_{2(3)}$. The function $G(\mathbf{q}, \Delta\varphi)$ describes the Bose-Einstein correlations and $K(\mathbf{q})$ is the Coulomb correction. In this analysis the Gaussian form of $G(\mathbf{q}, \Delta\varphi)$ was used [7]:

$$G(\mathbf{q}, \Delta\varphi) = \exp\Big[-q_{\text{out}}^2 R_{\text{out}}^2(\Delta\varphi) - q_{\text{side}}^2 R_{\text{side}}^2(\Delta\varphi) - q_{\text{long}}^2 R_{\text{long}}^2(\Delta\varphi) - 2q_{\text{out}}q_{\text{side}}R_{\text{os}}^2(\Delta\varphi) - 2q_{\text{side}}q_{\text{long}}R_{\text{sl}}^2(\Delta\varphi) - 2q_{\text{out}}q_{\text{long}}R_{\text{ol}}^2(\Delta\varphi)\Big], \tag{2}$$

where the parameters R_{out}, R_{side}, and R_{long} are traditionally called HBT radii in the *out*, *side*, and *long* directions. The cross-terms R_{os}^2, R_{sl}^2, and R_{ol}^2 describe the correlation in the *out-side*, *side-long*, and *out-long* directions, respectively.

$$R_{\mu}^2(\Delta\varphi) = R_{\mu,0}^2 + 2R_{\mu,n}^2\cos(n\Delta\varphi),\ R_{\text{os}}^2(\Delta\varphi) = R_{\text{os},0}^2 + 2R_{\text{os},n}^2\sin(n\Delta\varphi), \tag{3}$$

where μ = out, side, long, sl, and ol. Fitting the radii's azimuthal dependence with the functional form of Eq.3 allows us to extract the average radii and the amplitude of oscillations [8]. Figure 1 [8] shows the

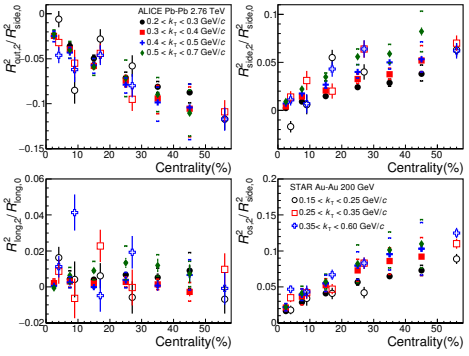

Fig. 1. Amplitudes of the relative radius oscillations $R_{\text{out},2}^2/R_{\text{side},0}^2$, $R_{\text{side},2}^2/R_{\text{side},0}^2$, $R_{\text{long},2}^2/R_{\text{long},0}^2$, and $R_{\text{os},2}^2/R_{\text{side},0}^2$ versus centrality for four k_{T} ranges. The error bars indicate the statistical uncertainties and the square brackets show the systematic errors. The STAR data points, for 0–5%, 5–10%, 10–20%, 20–30% and 30–80% Au–Au collisions [9], are slightly shifted for clarity.

relative amplitudes of the radius oscillations $R_{\text{out},2}^2/R_{\text{side},0}^2$, $R_{\text{side},2}^2/R_{\text{side},0}^2$, $R_{\text{long},2}^2/R_{\text{long},0}^2$, and $R_{\text{os},2}^2/R_{\text{side},0}^2$. We

observe similar results to that of STAR, however the STAR results [9, 10] show on average larger oscillations for $R^2_{\rm side}$. Our relative amplitudes for $R^2_{\rm out,2}/R^2_{\rm side,0}$, $R^2_{\rm side,2}/R^2_{\rm side,0}$, and $R^2_{\rm os,2}/R^2_{\rm side,0}$ show a clear centrality dependence, whereas the $R^2_{\rm long,2}/R^2_{\rm long,0}$ is very close to zero for all centralities, similarly to the results from RHIC [9].

The final source eccentricity at freeze-out $\varepsilon_{\rm final}$ can be estimated with an accuracy within 20–30% as $\varepsilon_{\rm final} \approx 2R^2_{\rm side,2}/R^2_{\rm side,0}$ [11]. Figure 2 [8] presents $2R^2_{\rm side,2}/R^2_{\rm side,0}$ for different $k_{\rm T}$ ranges as a function of the initial-state eccentricity for six different centralities. We find a smaller final-state anisotropy in the LHC regime compared to RHIC energies [12, 9]. The final-state eccentricity remains positive also at the LHC, evidence of an out-of-plane elongated source at freeze-out. In Fig. 2, we also compare our results to the 3+1D hydrodynamic calculations [13], this model slightly underestimates the final source eccentricity.

Figure 3 shows the relative amplitudes of the radius oscillations $R^2_{\rm out,3}/R^2_{\rm side,0}$, $R^2_{\rm side,3}/R^2_{\rm side,0}$, and $R^2_{\rm os,3}/R^2_{\rm side,0}$.

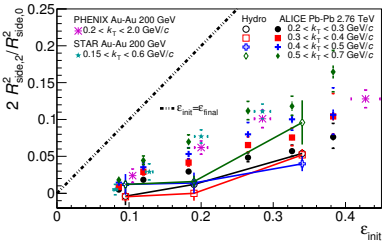

Fig. 2. An estimate of freeze-out eccentricity $2R^2_{\rm side,2}/R^2_{\rm side,0}$ for different $k_{\rm T}$ ranges vs. initial state eccentricity from Monte Carlo Glauber model [14] for six centrality ranges, 0–5%, 5–10%, 10–20%, 20–30 %, 30–40 %, and 40–50% from ALICE compared to RHIC results [12, 9] and 3+1D hydrodynamical calculations [13]. Square brackets indicate systematic errors.

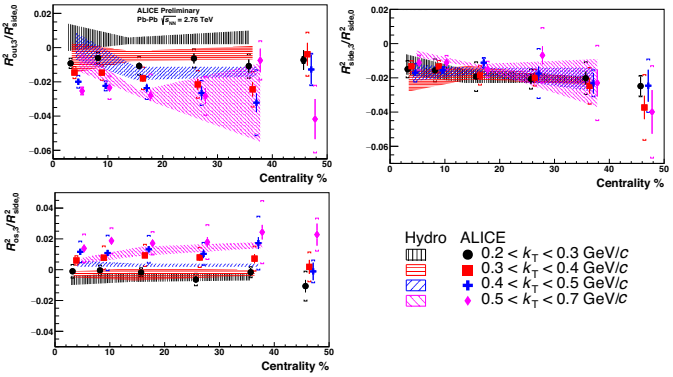

Fig. 3. Amplitudes of the relative radii oscillations $R^2_{\rm out,3}/R^2_{\rm side,0}$, $R^2_{\rm side,3}/R^2_{\rm side,0}$, and $R^2_{\rm os,2}/R^2_{\rm side,0}$ versus centrality for the $k_{\rm T}$ ranges 0.2–0.3, 0.3–0.4, 0.4–0.5, and 0.5–0.7 GeV/c. The shaded bands are the 3+1D hydrodynamical calculations. Square brackets indicate systematic errors.

The relative amplitudes for $R^2_{\rm out,3}/R^2_{\rm side,0}$ and $R^2_{\rm side,3}/R^2_{\rm side,0}$ have negative values for all centralities and $k_{\rm T}$ cuts. We compare our results with the 3+1D hydrodynamic calculations [13], where the relative amplitudes $R^2_{\rm side,3}/R^2_{\rm side,0}$ and $R^2_{\rm os,2}/R^2_{\rm side,0}$ agree quantitatively, and the relative amplitudes $R^2_{\rm out,3}/R^2_{\rm side,0}$ agree qualitatively with the 3+1D hydrodynamical calculations [13]. The relative amplitudes of the third harmonic results exhibit weak centrality and $k_{\rm T}$ dependence. According to the 3+1D hydrodynamical calculations, the negative signs of oscillations of R_{out} and R_{side} are an indication that the initial triangularity has been washed-out or even reversed due to the triangular flow.

In the event shape engineering analysis, events were selected based on the magnitude of the second

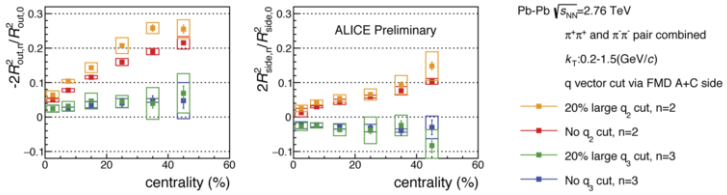

Fig. 4. Amplitudes of the relative radius oscillations $R^2_{\mathrm{out},2}/R^2_{\mathrm{side},0}$ ($R^2_{\mathrm{out},3}/R^2_{\mathrm{side},0}$) and $R^2_{\mathrm{side},2}/R^2_{\mathrm{side},0}$ ($R^2_{\mathrm{side},3}/R^2_{\mathrm{side},0}$) versus centrality with and without large q_2 (q_3) selection.

(third) order flow vector q_2 (q_3) [4], the Forward Multiplicity detector (FMD) was used to select on the magnitude of the flow vectors (-3.4 < η_{FMDC} < -1.7, 1.7 < η_{FMDC} < 5). We studied the effect of selecting the top 20% of the flow vector q_2 (q_3) on the magnitude of the flow v_2 (v_3). An enhancement of about 25% (15%) for v_2 (v_3) was observed for all centralities. Figure 4 shows the effect of large q_2 (q_3) selection on the relative amplitudes of the radii oscillations $R^2_{\mathrm{out},2}/R^2_{\mathrm{side},0}$ ($R^2_{\mathrm{out},3}/R^2_{\mathrm{side},0}$) and $R^2_{\mathrm{side},2}/R^2_{\mathrm{side},0}$ ($R^2_{\mathrm{side},3}/R^2_{\mathrm{side},0}$). The large q_2 selection significantly enhances the relative amplitudes of the radius oscillations $R^2_{\mathrm{out},2}/R^2_{\mathrm{side},0}$ and slightly enhanced $R^2_{\mathrm{side},2}/R^2_{\mathrm{side},0}$, possibly selecting more elliptic initial source. However, the large q_3 selection doesn't affect the relative amplitudes of the radius oscillations.

3. Summary

We have performed a measurement of two-pion azimuthally differential femtoscopy relative to the second and third harmonic flow plane in Pb–Pb collisions at $\sqrt{s_{\mathrm{NN}}} = 2.76$ TeV. The final-state source eccentricity is noticeably smaller than at lower collisions energies, but still exhibits an out-of-plane elongated source at freeze-out even after a stronger in-plane expansion. The negative signs of the relative amplitudes of radii oscillation, R_{out} and R_{side}, measured relative to the third harmonic flow plane, are an indication that the initial triangularity is washed-out or even reversed according to the 3+1D hydrodynamic calculations. The azimuthally differential HBT combined with ESE measurements were performed. The large q_2 selection has significant enhancement on the HBT radii relative to the second harmonic flow plane, whereas large q_3 selection has no effect on the HBT radii relative to the third harmonic flow plane.

Acknowledgement

This material is based upon work supported by the U.S. Department of Energy Office of Science, Office of Nuclear Physics under Award Number DE-FG02-92ER-40713.

References

[1] S. A. Voloshin, J. Phys. G38 (2011) 124097. arXiv:1106.5830, doi:10.1088/0954-3899/38/12/124097.
[2] G. Bertsch, M. Gong, M. Tohyama, Phys. Rev. C37 (1988) 1896–1900. doi:10.1103/PhysRevC.37.1896.
[3] S. A. Voloshin, W. E. Cleland, Phys. Rev. C53 (1996) 896–900. arXiv:nucl-th/9509025, doi:10.1103/PhysRevC.53.896.
[4] J. Schukraft, A. Timmins, S. A. Voloshin, Phys. Lett. B719 (2013) 394–398. arXiv:1208.4563, doi:10.1016/j.physletb.2013.01.045.
[5] A. M. Poskanzer, S. A. Voloshin, Phys. Rev. C58 (1998) 1671–1678. arXiv:nucl-ex/9805001, doi:10.1103/PhysRevC.58.1671.
[6] S. Pratt, Phys. Rev. D33 (1986) 1314–1327. doi:10.1103/PhysRevD.33.1314.
[7] S. Pratt, T. Csörgő, J. Zimányi, Phys. Rev. C 42 (1990) 2646–2652. doi:10.1103/PhysRevC.42.2646.
[8] D. Adamova, et al.arXiv:1702.01612.
[9] J. Adams, et al., Phys. Rev. Lett. 93 (2004) 012301. arXiv:nucl-ex/0312009, doi:10.1103/PhysRevLett.93.012301.
[10] J. Adams, et al., Phys. Rev. C71 (2005) 044906. arXiv:nucl-ex/0411036, doi:10.1103/PhysRevC.71.044906.
[11] F. Retiere, M. A. Lisa, Phys. Rev. C70 (2004) 044907. arXiv:nucl-th/0312024, doi:10.1103/PhysRevC.70.044907.
[12] A. Adare, et al., Phys. Rev. Lett. 112 (2014) 222301. arXiv:1401.7680, doi:10.1103/PhysRevLett.112.222301.
[13] P. Bozek, Phys. Rev. C89 (2014) 044904. arXiv:1401.4894, doi:10.1103/PhysRevC.89.044904.
[14] S. Ghosh, S. K. Singh, S. Chatterjee, J. Alam, S. Sarkar, Phys. Rev. C93 (2016) 054904. arXiv:1601.03971, doi:10.1103/PhysRevC.93.054904.